International Journal of Chemical, Materials and Biomolecular Sciences
ISSN: 2415-6620
Vol:12, No:5, 2018

# A Simplified, Fabrication-Friendly Acoustophoretic Model for Size Sensitive Particle Sorting

V. Karamzadeh, J. Adhvaryu, A. Chandrasekaran, M. Packirisamy

***Abstract*—**In Bulk Acoustic Wave (BAW) microfluidics, the throughput of particle sorting is dependent on the complex interplay between the geometric configuration of the channel, the size of the particles, and the properties of the fluid medium, which therefore calls for a detailed modeling and understanding of the fluid-particle interaction dynamics under an acoustic field, prior to designing the system. In this work, we propose a simplified Bulk acoustophoretic system that can be used for size dependent particle sorting. A Finite Element Method (FEM) based analytical model has been developed to study the dependence of particle sizes on channel parameters, and the sorting efficiency in a given fluid medium. Based on the results, the microfluidic system has been designed to take into account all the variables involved with the underlying physics, and has been fabricated using an additive manufacturing technique employing a commercial 3D printer, to generate a simple, cost-effective system that can be used for size sensitive particle sorting.

***Keywords*—**3D printing, 3D microfluidic chip, acoustophoresis, cell separation, MEMS, microfluidics.

## I. Introduction

OVER the last decade, the use of the ultrasonic field for the separation, positioning, handling and characterization of microparticles, cells and droplets has been remarkably increased [1]. Force inducted by an acoustic field leads to the movement of microparticles, namely acoustofluidics, enable mechanical manipulation of particle and cell in microfluidic channels [2].

In acoustophoresis, the prediction of the acoustic streaming is essential before design and fabrication. However, the development of these devices is hindered due to fabrication restrictions. In BAW microfluidics, the efficiency of particle sorting is determined by factors, such as the geometry of the channel and the properties of the fluid medium. Therefore, obtaining an accurate model is essential to understand the physics of the system prior to fabrication of the system.

Conventional methods to fabricate microfluidic devices are mostly based on surface and bulk micromachining. However, achieving to 3D microchannels with these methods is not feasible.

Recently, 3D printing became an alternative technology to fabricate microfluidic devices [3]-[6]. However, the problem with this method is mostly the resolution of the 3D printed part which is not suitable for most of these applications. Since in acoustofluidics devices, channel size is in the order of 100 microns 3D printing could be a promising fabrication method for developing these devices [1], [7]-[11]. Moreover, the throughput of sorting is dependent on the aspect ratio of the channel. Since attaining 3D channel is accessible with additive manufacturing methods, this low-cost fabrication method could make the fabrication accessible and cheaper. To best of our knowledge, to date, fabrication of acoustofluidics devices have not been reported using 3D.

Here, we suggest a simplified Bulk acoustophoretic system fabricated using a 3D printed mold in order to achieve 3D channels that can be used for size dependent particle sorting.

## II. Theoretical Background

The acoustic radiation force from scattering of acoustic wave and the acoustic velocity field of the fluid play a key role in an acoustophoresis system. These forces and the regime affect particles and they either move to walls or stay at the corner of the channel.

Acoustic radiation and acoustic streaming are induced in the microfluidic channel by a piezo-electric resonator. These forces help to manipulate or to focus the particles/cells in the microfluidics environment.

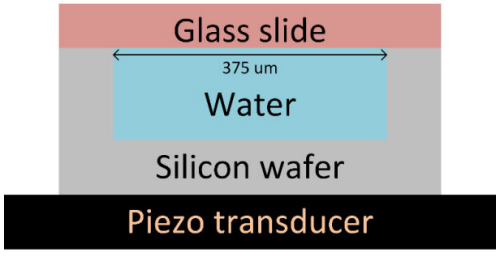


Fig. 1 Depiction of the acoustophoresis device

As a consequence of acoustic field, acoustic streaming occurs in the microfluidic channel which is the bulk of the liquid rotation. When the particles are injected into the microfluidic channel, particle also moves with the rotating bulk liquid which restricts particle to be focused in the center of the channel. Another force which is induced due to scattering of ultrasound standing wave is acoustic radiation

V. Karamzadeh is with the Optical-Bio Microsystems Laboratory, Department of Mechanical and Industrial Engineering, Concordia University, Montreal, Quebec, H3G 1M8, Canada (e-mail: v_karamz@encs.concordia.ca).

J. Adhvaryu is with the Department of Mechanical and Industrial Engineering, Concordia University, Montreal, Quebec, H3G 1M8, Canada (e-mail: j_adhvar@encs.concordia.ca).

A. Chandrasekaran is with the Cellular Microenvironment Design Lab, Department of Chemical Engineering, McGill University, Montreal, Quebec, H3A 0C5, Canada (e-mail: arvind.chandrasekaran@mcgill.ca).

M. Packirisamy is with the Optical-Bio Microsystems Laboratory, Department of Mechanical and Industrial Engineering, Concordia University, Montreal, Quebec, H3G 1M8, Canada (phone: +1-514-8482424 #7973; fax: +1-514-8483175; e-mail: mpackir@encs.concordia.ca).

force. This force helps particle to move towards the node of the ultrasound standing wave. Therefore, radiation force has to overcome the drag force in order to focus particles to the center of the channel.

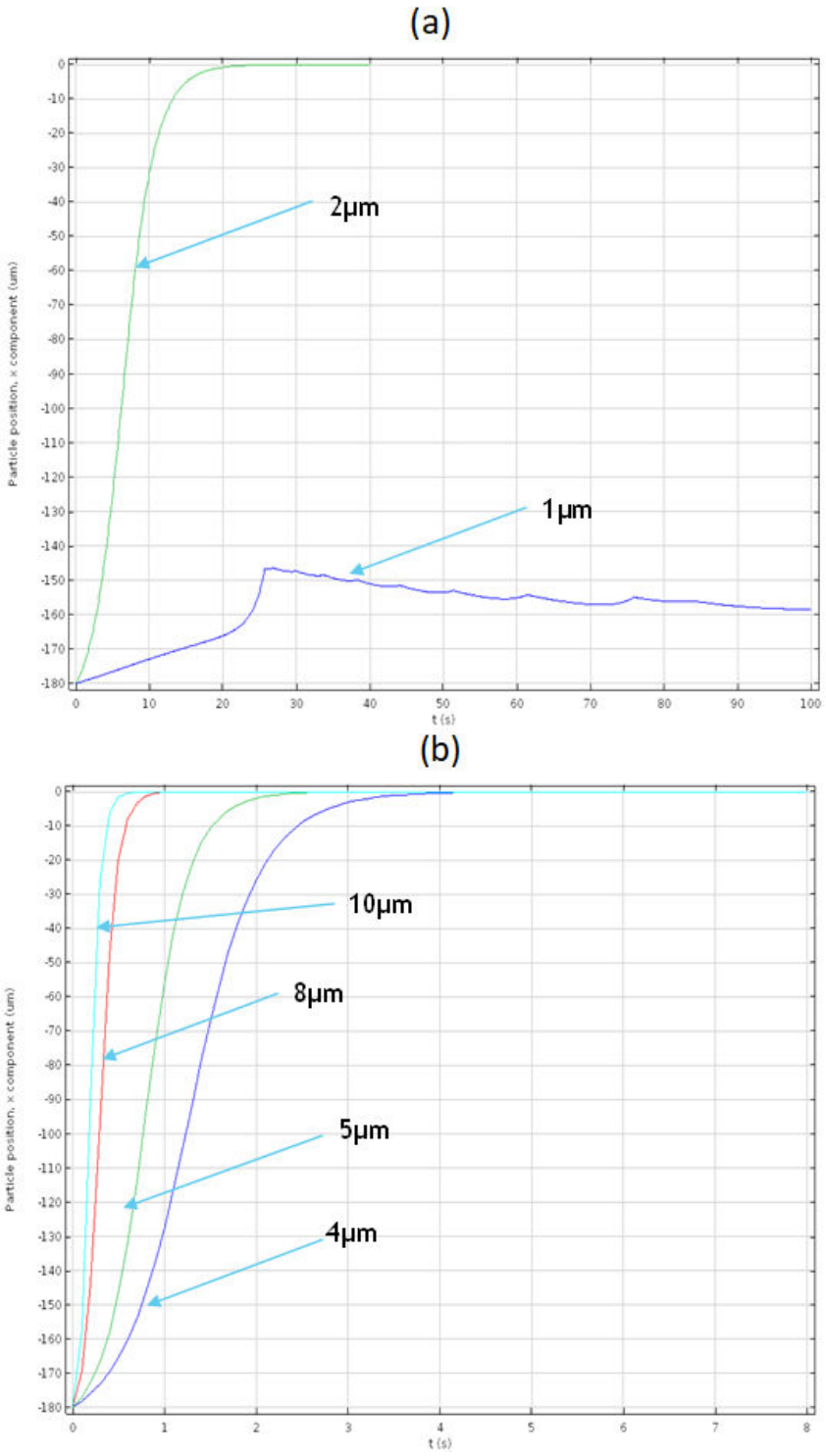


Fig. 2 Particle position verses time; (a) 2$\mu m$ and 1 $\mu m$; (b) 4 $\mu m$, 5 $\mu m$, 8 $\mu m$ and 10 $\mu m$

*A. Variation of Particle Diameter*

Since acoustic focusing method by BAW is highly dependent on the diameter of the particle, it is imperative to analyze what happens when the diameter of the particle is

altered. From this study, the strength and the limitation of the BAW can be identified.

Numerical simulation is employed in COMSOL V 5.2 by varying particle diameter. The range of the particle diameter is 1, 2, 4, 5, 8 and 10 μm. As can be seen from Fig. 2 (a), 2 μm particle can be manipulated to the center of the channel. However, the applied force is not effective on 1 μm particle. The reason behind this is 1 μm particle is small that it cannot able to experience acoustic radiation force. Furthermore, to focus particles to the center of the channel, acoustic radiation force must overcome the drag force induced by acoustic streaming. In this case, 1 μm particles are primary streaming dominated means acoustic radiation force is not large enough to overcome the drag force.

As illustrated in Fig. 2 (b) when the diameter of the particle is increased, it experienced more acoustic radiation force compared to smaller diameter particle. Therefore, that retention time also decreases as the diameter of the particle is increased. This concept is also verified from Fig. 3 that as the diameter of the particle is decreased, retention time reduces exponentially.

The critical diameter of the particle is calculated form the condition $F_{rad} = F_{drag}$ which means when the acoustic radiation force is equal to the drag force produced by acoustic streaming, particle will stop moving further [8]. If the particle has a diameter less than critical diameter it is not able to experience acoustic radiation force and it is totally acoustic streaming dominated. The critical diameter is given by:

$$D_c = 2\,a_c = \sqrt{\frac{12\psi}{\phi}}\,\delta = 1.97\mu m \approx 2\mu m \quad (1)$$

One of the limitations of the BAW is not being able to separate particle less than 2 μm.

*B. Variation of Aspect Ratio (H/W)*

Since resonance is depending on the width of the channel, it was considered as constant but height is an independent variable. Aspect ratio is the ratio of height to width of the channel.

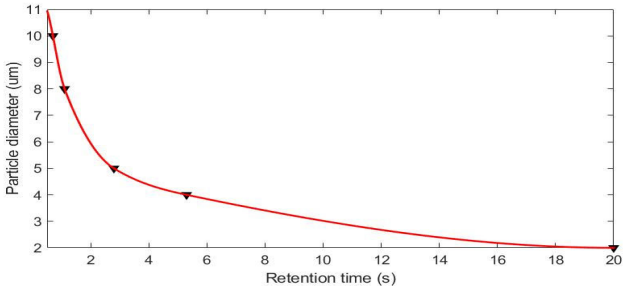


Fig. 3 Particle diameter verses retention time

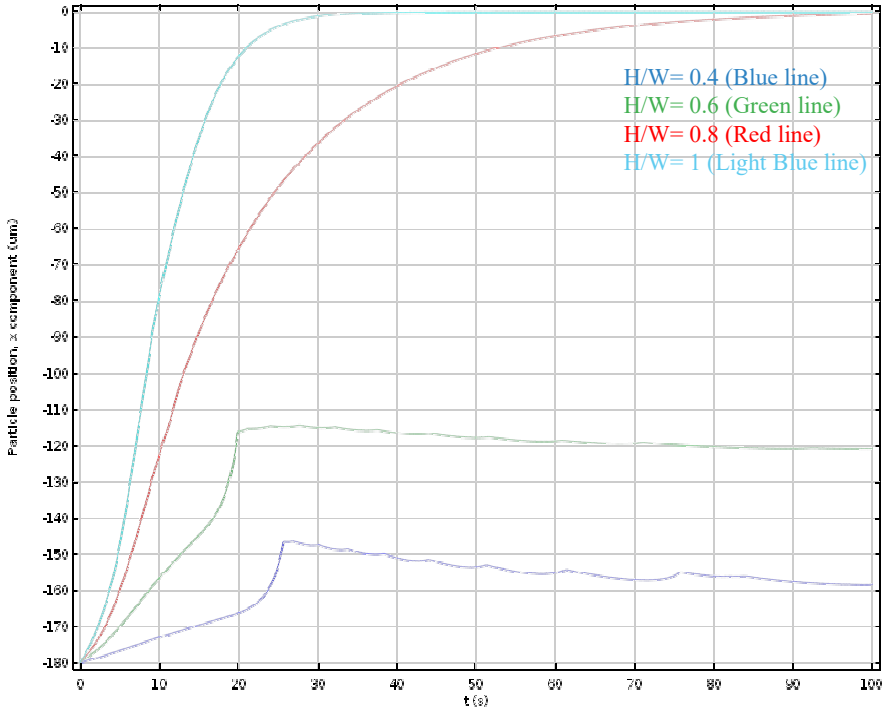


Fig. 4 1 μm particle position verses time for different aspect ratios

In this study, four range of aspect ratio are used for the study starting form H/W=0.4 to H/W=1 with 0.2 step. As shown in Fig. 4, focusing of the particle is possible for the aspect ratio H/W more than 0.8. The particle is totally dominated by the acoustic streaming for an aspect ratio less than 0.8. However, particles were focused with an aspect ratio

of more than 0.8. When the height of the channel is increased, the strength of the streaming velocity is decreased so that drag force which is induced by acoustic streaming is reduced but it does not mean that radiation force is increased. Actually, now drag force is inadequate that acoustic radiation force overcomes the drag force and focusing of the particle is possible.

The same concept is applicable for all particles. That is why retention time for all particles is decreased due reduction in the drag force. Therefore, it is one of the methods which provide a remedy to the limitation of a bulk acoustic wave system.

### *C. Variation of Amplitude Ratio*

Here, the impact of the amplitude ratio on the particle focusing is studied. Since, amplitude is directly related to actuation energy, it is interesting to see its impact and come to some significant conclusion.

As can be seen from Fig. 5 (a), by increasing the actuation energy, there is not any impact on particle focusing in case of a particle with less than 2 μm diameter. As we increase the amplitude, acoustic radiation force increases. Therefore, referred to Fig. 5 (a), it seems that it does not focus even with higher acoustic radiation force. Because, with acoustic radiation force, acoustic streaming force increases. Therefore, drag force also increases and particles cannot be focused.

For particles with a higher diameter as we can see form the Fig. 5 (b), retention time decreases significantly due to higher radiation force.

## III. Fabrication

As discussed in the previous section, the efficiency of the device is highly dependent on the aspect ratio of the channel. Using a 3D printed mold leads to achieve a 3D channel in order to find an optimum aspect ratio for the system according to the width of the channel. The CAD model of the mold with 375 $\mu m$ width and a variant aspect ratio between 0.4 to 1.2 was designed using Solidworks (Dassault Systèmes). The designed model was exported as an STL file and printed using Formlabs 2 which is a SLA 3D printer. Printing of each part takes approximately 135 min. The resolution of the 3D printer according to its datasheet is 150 μm in the XY plane and 25 μm in the Z axis. A base thickness of 2 mm was considered to prevent the model from bending.

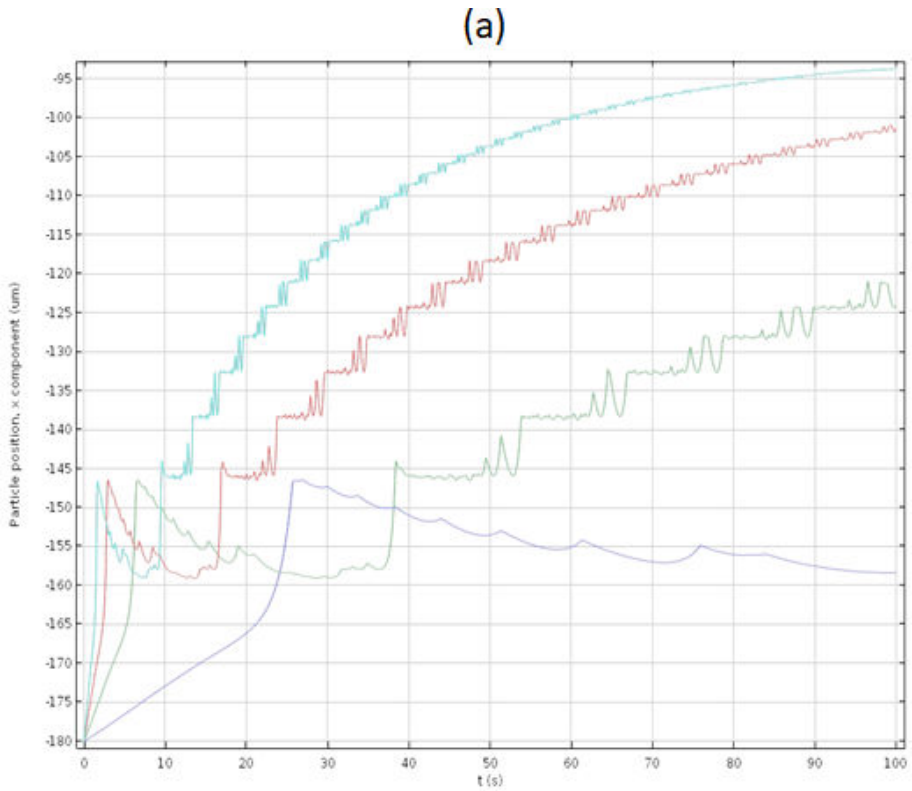

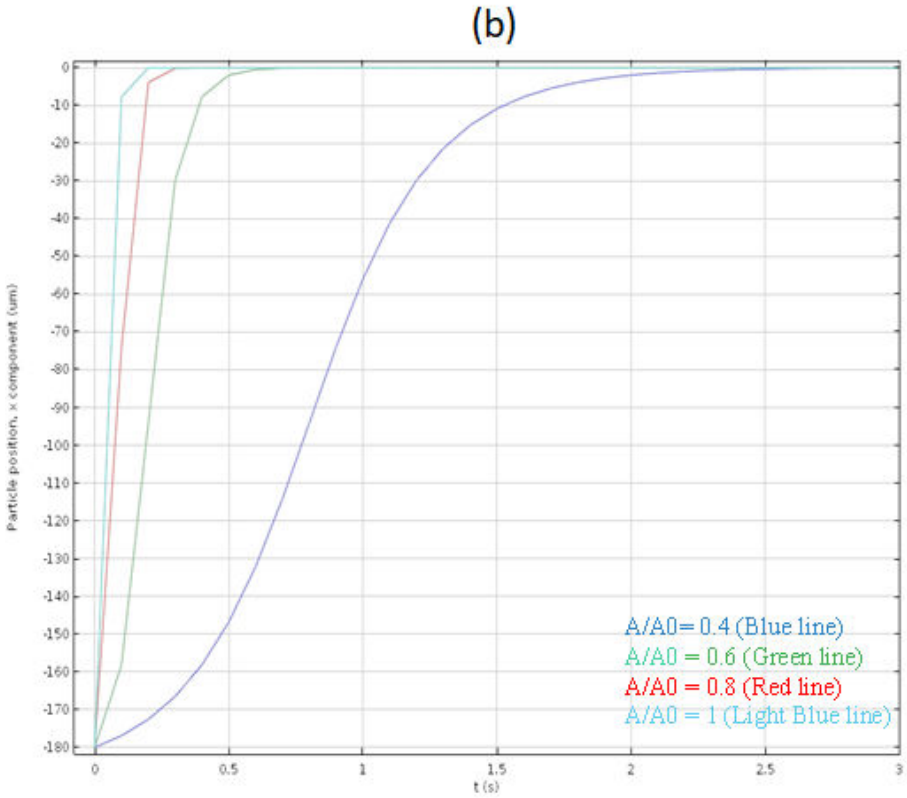


Fig. 5 Particle position verses time for variety of amplitude ratio; (a) particle size equals 1 µm; (b) particle size equals 5 µm

The 3D printed mold was washed with isopropanol for 2 minutes after printing and then nitrogen gas was used to dry it and then it was exposed to UV light (Stratalinker® UV Crosslinker 2400) for 6 min. The molds' accuracy and roughness were inspected using confocal microscopy. Surface profile was attained by using a Confocal Laser Scanning Microscope (Olympus Inc.). Area of 2.4 mm by 1.2 mm was scanned with the ultrafine setting. The scanning of this area takes 60 min. Since the PDMS cannot be polymerized into a cured part in contact with the surface of the molds, they are treated with oxygen plasma at high power (Harrick Plasma, Inc.) before molding for two minutes and then the parts are coated with fluorinated silane (Trichlorosilane, Sigma-Aldrich, Inc.) for 6 hours at 60 °C. Consequently, the cured parts will be removed easily from the master mold and the surface will not be sticky [12].

PDMS components were purchased from Dow Corning Crop (USA). Mixed polymer at 10:1 ratio (w/w) degassed in a vacuum chamber for 30 min prior to casting. Then, the polymer was poured into the printed mold. The PDMS was cured in an oven at 70 °C for 4 hours. Afterwards, the PDMS part was peeled off from the master mold and cleaned with IPA. The required holes for fluid inlet and outlet were made prior to plasma treating and thereafter, a glass slide and the PDMS part were treated with oxygen plasma for 50 sec and were bonded to each other. A piezoelectric actuator was placed on the glass slide.

## IV. Conclusion

The FEM was successfully implemented using COMSOL 5.2 to model BAW for particle manipulation/separation in a microfluidic channel. Thermo-acoustic module, laminar flow module and particle tracing module were used to analyze the mechanism of BAW. The physics behind the BAW is studied in detail. The dependence of the system to different parameters such as the particle size, aspect ratio of the channel and amplitude ratio was investigated in this work. The limitation of BAW is also studied and remedy for it is also offered by varying aspect ratio of the channel which helps to reduce drag force due to acoustic streaming significantly. In order to overcome this limitation, using 3D printed mold was suggested to achieve a channel with a variant aspect ratio through the channel. This fabrication method leads to cost and time effective fabrication compared to cleanroom-based microfabrication methods.

## References

[1] I. Leibacher, S. Schatzer, and J. Dual, "Impedance matched channel walls in acoustofluidic systems," *Lab Chip*, vol. 14, no. 3, pp. 463–470, 2014.

[2] C. W. Shields IV, C. D. Reyes, and G. P. López, "Microfluidic cell sorting: a review of the advances in the separation of cells from debulking to rare cell isolation," *Lab Chip*, vol. 15, no. 5, pp. 1230–1249, 2015.

[3] G. Comina, A. Suska, and D. Filippini, "PDMS lab-on-a-chip fabrication using 3D printed templates," *Lab Chip*, vol. 14, no. 2, pp. 424–430, 2014.

[4] R. Amin, S. Knowlton, A. Hart, B. Yenilmez, and F. Ghaderinezhad, "3D-printed microfluidic devices," *Biofabrication*, vol. 8, no. 2, pp. 1–16.
[5] A. Ahmadian, Y. Adam, P. William, and W. Tammy, "3D printing : an emerging tool for novel microfluidics and lab-on-a-chip applications," *Microfluid. Nanofluidics*, 2016.
[6] S. Waheed *et al.*, "3D printed microfluidic devices: enablers and barriers," *Lab Chip*, vol. 16, no. 11, pp. 1993–2013, 2016.
[7] I. Leibacher, P. Reichert, and J. Dual, "Microfluidic droplet handling by bulk acoustic wave (BAW) acoustophoresis," *Lab Chip*, vol. 15, no. 13, pp. 2896–2905, 2015.
[8] P. B. Muller, R. Barnkob, M. J. H. Jensen, and H. Bruus, "A numerical study of microparticle acoustophoresis driven by acoustic radiation forces and streaming-induced drag forces," *Lab Chip*, vol. 12, no. 22, p. 4617, 2012.
[9] M. Antfolk, P. B. Muller, P. Augustsson, H. Bruus, and T. Laurell, "Focusing of sub-micrometer particles and bacteria enabled by two-dimensional acoustophoresis," *Lab Chip*, vol. 14, no. 15, pp. 2791–2799, 2014.
[10] P. Augustsson, J. T. Karlsen, and H. Bruus, "Acoustophoretic manipulation of sub-micron objects enabled by density gradients," in *20th International Conference on Miniaturized Systems for Chemistry and Life Sciences, MicroTAS 2016*, 2016, pp. 158–159.
[11] P. Augustsson, J. T. Karlsen, H.-W. Su, H. Bruus, and J. Voldman, "Iso-acoustic focusing of cells for size-insensitive acousto-mechanical phenotyping.," *Nat. Commun.*, vol. 7, no. May, p. 11556, 2016.
[12] H. N. Chan, Y. Chen, Y. Shu, Y. Chen, Q. Tian, and H. Wu, "Direct, one-step molding of 3D-printed structures for convenient fabrication of truly 3D PDMS microfluidic chips," *Microfluid. Nanofluidics*, vol. 19, no. 1, pp. 9–18, 2015.